



A PI Controller based MPPT For PV System under PSC using AVI-CO Approach

Meher Pratham Achampetkar

Lamar University, Beaumont, Texas, United States.

Abstract: This paper presents a novel AVI-CO technique based MPPT controller for PV systems under unshaded, partially shaded and fully shaded scenarios. The gains demonstrated by the suggested approach include a rise in PV system reliability, quick and accurate GM tracking and extremely small GM fluctuations. Similarly, to overcome the shortcomings associated with intelligent and standard MPPT techniques, including PS loss of power, GM tracking effectiveness, fluctuations, and steady power output, a meta-heuristic optimization based MPPT is proposed. In such circumstances, where the minimal DC voltage at the input must be transformed to a larger DC voltage at the output, the high-power step-up DC-DC conversion process encounters rising needs and power capacity requirements. By regulating the duty cycle with the aid of a PI controller, regulation of the output voltage in the DC-DC converter can be accomplished. The PI controller parameters, K_p and K_i are tuned by employing the developed Adaptive variable Insisted Coyote Optimization (AVI-CO) Approach that helps to provide better performance. The anticipated research is simulated in MATLAB/Simulink and their experimental investigation is carried out. The examination under three shaded scenarios is carried out to enhance the effectiveness of the arrangement compared to existing algorithms.

Keywords: DC/DC converter; Partial Shading; Solar PV panel; PI controller; Optimization.

Nomenclature

Abbreviation	
PSC	Partial Shading Conditions
PI	Proportional-Integral
IEA-PVs	International Energy Agency For PVs
PVs	Photovoltaic Power Systems
MPPT	Maximum Power Point Tracking
LMPP	Local MPP
GMPP	Global MPP
P&O	Perturb And observe
IC	Incremental Conductance
PSO	Particle Swarm Optimization
GWO	Grey Wolf Optimization
ABC	Artificial Bee Colony
CSO	Cuckoo Search Optimization
AVI-CO	Adaptive Variable Insisted Coyote Optimization
COA	Coyote Optimization Algorithm
PSO	Particle Swarm Optimization
GRNN-SFO	General Regression Neural Network Trained With The Sailfish Optimizer
SI	Swarm Intelligence
MPA	Marine Predator Algorithm
MFA	Mayfly Optimisation Algorithm
GTOA	Group Teaching Optimisation Algorithm
WO	Without Optimization
OBL	Opposition-Based Learning
CPS	Complex Partial Shading
SRA	Search And Rescue Algorithm
MBOA	Modified Butterfly Optimisation Algorithm

1. Introduction

Considering a daily basis, the population is growing and new technologies, like electric cars, power electronics, cutting-edge machinery, etc. are being developed, which is leading to an increase in the global energy demand [9][10]. The main reason why people are interested in renewable energy sources is because of various factors. Solar energy is given special consideration because of its sustainability, abundance, lack of pollution, and lack of carbon emissions. PV systems are used in over a hundred nations now for both stand-alone and grid-connected applications. According to IEA-PVPS' predictions, the installation of PV capacity all over the world is estimated to increase to 500 GW by the end of 2020 [11][12]. Temperature and irradiation levels affect the solar energy [13]. Operating the PV array at MPP is therefore very important, and the MPPT controller makes this feasible. Among the load and the PV supply, an electronic power converter is employed to enable MPPT. The solar PV system is comprised of solar arrays that are linked in series to provide a high-voltage input to the grid-dependent inverters.

Since the components are connected in series, they must all produce the same quantity of current. According to PSC, the module with shading cannot produce the same amount of current as the unshaded one [14]. So, contrary to the supply current, the shaded module will draw it. An avalanche breakdown may follow as a result, which may result in the development of a hotspot on the panel surface [15]. The P-V and I-V curves exhibit many peaks as a result of the parallel bypass diodes that are employed via the bypass-shaded modules to prevent the hotspot phenomena. Multiple MPPT strategies were suggested in the literature because MPPT is a popular study area. Common algorithms, such as P&O, hill climbing, and IncC [16], are easy-to-understand algorithms with quick tracking speeds. Nevertheless, the issues related to them include oscillation within the MPP, indirect control of the duty cycle necessitating an alteration of PID/PI variables, changes needed to modify the direction of the duty cycle perturbation with the switch from buck to boost converter, and their range of tracking is local search space [17][18][19][20]. This is a result of their method of attaining the MPP through voltage perturbation and power observation. In the event of a mismatch, the operating point continues to bounce over LMPP whenever it is located in the LMPP zone but is unable to search for the GMPP region. Additionally, bio-inspired methods, often referred to as meta-heuristic methods, such as PSO [21], GWO [22], CSO [23], and ABC [24], provide a workable way to track GMPP with a lot more efficiency. In addition, the optimization-based MPPT controller has the potential to improve the performance of several scientific challenges, which has sparked the interest of many academics in the hybrid algorithm.

The major contribution made by this paper is as follows:

- Introduces a PI controller so that the duty cycle can be adjusted to achieve output voltage regulation in the DC-DC converter.
- Introduces a novel meta-heuristic strategy termed Adaptive Variable Insisted Coyote Optimization (AVI-CO) approach, which helps to tune the PI controller parameters.
- Convergence and efficiency analysis are used to measure how well the developed work performs under different shading situations.

The paper is organized as follows: Section II describes the existing works based on MPPT. Section III designates the PV System Modelling and Behaviour under Uniform Irradiance and PS Conditions and section IV instructs the finest tuning of PI parameters by AVI-CO Approach. Section V represents the simulated findings. Section VI elucidates the results and section VII concludes the paper.

2. Literature Review

2.1 Related Works

In 2021, Muhammad Hamza Zafar, *et al.* [1] developed a brand-new MPPT-based SRA optimization technique to address the issues related to existing models of MPPT. The gains demonstrated by the suggested approach include an increase in PV system performance, quick and accurate GM tracking, and extremely small GM oscillations. The SRA was intended to address the shortcomings of intellectual and traditional MPPT methods, including PS power losses, effective GM tracking, fluctuations, as well as constant power output. The findings were analogized with these well-optimized and modern MPPT controllers, like GHO, GWO, PSO, PSOGA, and CSA. The suggested method was resilient because the tracking duration was from 60%-72% and the settling period was 180% quicker, respectively. The output voltage amplitude was far lower than 0.5 W, resulting in a steady transient. The least RMSE, MAE, and RE were attained with the maximum SR of GM tracking using the analytically suggested SRA-based MPPT controller.

In 2021, Essam H. Houssein *et al.*, [2] developed an innovative hybrid MPA method that utilizes GWO and MPAOBL-GWO techniques to monitor the global MPP obtained via the shaded PV module.

However, if contrasted with conventional meta-heuristic techniques, it would demonstrate the durability of the stated MPAOBL-GWO-based global MPPT. Additionally, the current study utilizes the smallest populace size to address the time-consuming challenge, which lessens the difficulty of GMPP. As a result, the recommended MPPT controller was less expensive since it only required a single sensor. The findings gained also demonstrate that the provided MPAOBL-GWO-based technique may achieve the best results when compared to the traditional MPA, GWO, and PSO methods.

In 2020, Immad Shams *et al.* [3] developed an innovative MPPT approach that utilizes MBOA, which can distinguish amongst various partial shade patterns, constant shading, solar intensity, and load variation circumstances with quick rapid convergence. The level of complication of the technique was diminished by employing a single dynamic component as a tuning variable. A search space-skipping solution was utilized to enhance the CS. To increase the system's response time for rapidly changing load conditions, the suggested method was hybridized with a constant impedance method. With a sample time of 0.05s, the suggested approach had been empirically verified on the SEPIC converter design. The field test verification demonstrated that the average time tracking for various shade arrangements is always less than 1 s, with an average steady-state accuracy of 99.85%. A 47.20% improvement was made to the CS under conditions of homogeneous shade. Additionally, by a factor of 86.15%, the reaction to load variation was enhanced and qualifies for use with rapidly changing load variations. To assess the efficacy of the suggested method, a list of comparisons based on the MPPT rating has been produced.

In 2021, N. Padmavathi *et al.* [4] provided a regression controller to monitor the PV modules' peak power at different PSCs. Additionally, the regression controller forecasts the boost converter duty cycle for short as well as long-term weak shadowing conditions. Furthermore, the regression controller appreciates PV voltages with shadow and necessitates duty cycle forecasts without uneasiness or difficult calculations. The analysis suggests that by creating a robust tie-up between PV solar voltage and the duty cycle of PWM, the suggested controllers can operate better than alternative approaches during step change and PSC. The regression controller arrives at MPP very quickly because of speedy computation. The speed of convergence rises due to fast changes in the PV cell duty cycle in response to solar irradiation at the greatest peaks.

In 2020, Muhammad Hamza Zafar *et al.* [5] developed an innovative GTOA-based controller that successfully manages the PS and CPS conditions. To assess the sturdiness of the suggested MPPT approach, four case studies with faster-changing irradiation, PS, and complex PS were used. The GTOA maintained the magnitude of the oscillation while tracking the global MPP with the greatest accuracy. Cases 2 and 3 for the PS condition as well as the unique case 4 for CPS were also involved. The approach had strong robustness and outperformed competing technologies regarding tracking speed, settling speed, power tracking effectiveness, and fluctuation reduction, according to experimental, analytical, and statistical analysis results.

In 2020, Maykon Vichoski da Rocha *et al.* [6] offered a comparison study of algorithms using MPPT focused on the Bat-based optimization method that can achieve the GMPP. Even with tiny differences in solar irradiation, the approach used by the majority of metaheuristic approaches to realize the GMPP, the scheme may display significant fluctuations in PV power. Therefore, configurations based on the Bat-based approach with typical algorithms, like P&O, Beta and IC were suggested to lessen power oscillations and increase the PV system performance. Utilizing a DC/DC Boost converter, the typical MPPT algorithms, like Bat-Beta, Bat-IC and Bat-P&O were assessed and contrasted with one another. At last, the efficacy of the created systems was appraised using tentative findings and simulated data.

In 2021, Muhammad Hamza Zafar *et al.* [7] presented two innovative MPPT algorithms that utilize SI, the MPA and the MFA to maximize power amid rapidly varying irradiance, PSC, and complex PSC. MPPT control was the most effective approach to increase the output PV system power under unchanging and irregular irradiation stages. In comparison to PSO, GWO, CS, GHO and P&O, findings demonstrate that the suggested MPPT approaches can monitor the GM with 99.9% efficacy and with 20%–50% quick tracking time. The suggested approach minimizes oscillation at the GM by as much as 97% in comparison to the traditional MPPT-based P&O methodology. A research investigation demonstrates that the recommended strategies were more robust and stable than the alternatives. The suggested method generates cleaner energy because of its fast-tracking capacity, excellent power effectiveness, and effective harvesting of energy.

In 2021, Noman Mujeeb Khan *et al.* [8] described an integrated MPPT technique that was built using a GRNN-SFO. The GRNN-SFO was extremely an efficient global optimization of the sailfish optimizer that was paired accurately with estimated capacity. To prove that GRNN-SFO functions better than other algorithms, two scenarios were shown. When irradiance was rapidly changing and there was partial shadowing, the assessment demonstrates that GRNN-SFO follows the GMPP with 99.9%

effectiveness and also with a quick tracking speed of 12 ms. The statistical data evaluation was additionally placed on display to assess the durability and adaptability of the suggested approach.

2.2 Problem Definition

The investigations on various optimization-based MPPT controllers for PV systems at PSCs are disclosed in Table 1. Initially, an SRA-based MPPT strategy was introduced in [1], which offers more robustness with better power tracking efficiency of 99.93%; however, the problem occurs due to non-efficient tracking that may cause more power loss. An MPAOBL-based GWO strategy in [2] attains optimum solution with better efficiency; moreover, it needs consideration of real-world applications for solving partial shading problems. MBOA strategy was introduced in [3] which requires a single parameter depending on V_{oc} of a PV panel which makes the simulation simpler. Nevertheless, During the mismatch scenario, it was not able to scan under the GMPP region. A Regression controller-based MPPT was presented in [4], which requires less time to converge and possesses high convergence speed; however, it undergoes a major drawback of complex computation. A GTOA-based MPPT was created in [5], which possesses a high efficacy of 99.9% as well as it traces GMPP within 140 ms. However, the accuracy is not reliable. A bat-MPPT algorithm was developed in [6], which minimizes power oscillations and enhances PV performance. Moreover, there occurs a major drawback of early convergence, so it is difficult to obtain better optimization results. An MPA and MFA-based MPPT was presented in [7], which can track fast with high energy efficacy. However, MFA takes more computation time. A GRNN-SFO approach was introduced in [8] which attains efficacy >99.9% and also tracks GM within 12 ms. However, they have their flaws, particularly their intricacy and it is difficult to implement them in the real world.

Table 1: Assessment of existing methods of MPPT controllers under PSC

Author [citation]	Adopted methodology	Features	Challenges
Muhammad Hamza Zafar, <i>et al.</i> [1]	SRA based MPPT Strategy	Power tracking efficacy of 99.93%. More robust	Ineffective tracking may contribute to increased power loss, which is the real problem.
Essam H. Houssein <i>et al.</i> , [2]	MPAOBL based GWO Strategy	Accomplish optimal results. Improved efficacy.	Focus should be given to practical applications for fixing partial shading issues.
Immad Shams <i>et al.</i> [3]	MBOA approach	Require a single parameter depending on V_{oc} of a PV panel which makes the simulation simpler.	During the mismatch scenario, it is not able to scan under the GMPP region.
N. Padmavathi <i>et al.</i> [4]	Regression Controller based MPPT	Need lesser converge time. Increases convergence speed.	Complex Computation
Muhammad Hamza Zafar <i>et al.</i> [5]	GTOA based MPPT	Efficiency is 99.9%. Trace GMPP within 140ms.	Accuracy is not reliable.
Maykon Vichoski da Rocha <i>et al.</i> [6]	Bat-MPPT Algorithm	Minimize power oscillations. Enhance PV performance.	There occurs a major drawback of early convergence, so it is difficult to obtain better optimization results.
Muhammad Hamza Zafar <i>et al.</i> [7]	MPA & MFA based MPPT	Ability to track fast. High energy efficacy.	MFA take more time to compute.
Noman Mujeeb Khan <i>et al.</i> , [8]	GRNN-SFO approach	Efficacy >99.9%. Tracks GM within 12ms.	However, they have their flaws, particularly their intricacy and it is difficult to implement them in the real world.

3. PV System Modelling and Behaviour under Uniform Irradiance and PS Conditions

3.1 PV cell Modelling

It is preferable to represent the PV cell using an anti-parallel diode with a DC source. A PV cell is realistically modelled by adding parallel as well as series resistances, termed R_{sc} and R_p . The single-diode model is a straightforward estimator of a PV cell that improperly disregards the impact of external factors on P-V and I-V curves. Fig. 1 depicts a single diode model that is employed to accurately model

the PV cell. A more functional version of the double diode PV model of [25] is shown by dual anti-parallel diodes having a DC source with series-parallel resistance. Eqs. (1) and (2) describe the single-diode PV system's statistical modelling.

$$I_t = I_{spv} - I_{diode} \quad (1)$$

$$I_t = I_{spv} - I_{sc} \left(\exp \left(\frac{V_o}{\delta V_t} \right) - 1 \right) \quad (2)$$

$$I_t = I_{spv} - I_{sc} \left(\exp \left(\frac{V_o + I_t R_{se}}{\delta V_t} \right) - 1 \right) \quad (3)$$

$$V_t = \frac{N_{sc} k t}{q} \quad (4)$$

Whereas, V_o and I_t are the output voltage as well as output current; I_{spv} be the generated PV current, and it is directly proportional to the light incidence. Eqn. 1 shows the current (I_t) flowing about output via the diode (I_{diode}) as it passes through it. δ is the ideality factor of the diode; N_{sc} defines the cell count in series; V_t denotes the thermal voltage; R_{se} and R_p signifies the series and parallel resistances, respectively.

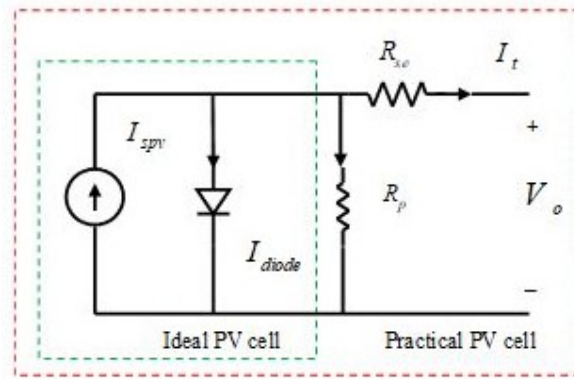


Fig. 1. Single diode Model of a Solar PV cell

3.2 Under Partial Shading Scenario

Partial shading happens when light with varying irradiance strikes a row of interconnected modules. PV systems must run at their maximum output point, which varies depending on the environmental variables, such as temperature or irradiation levels, to attain the highest efficiency. Nevertheless, certain panels may decrease voltage and begin to act resembling a load owing to non-uniform irradiation phases. Six seriously linked PV panels under uniform irradiance are illustrated in Fig. 2. This is because many PV panels have to be linked in series as well as parallel arrangements for more power generation. The maximum power point for an evenly distributed irradiance level is represented by the I-V and P-V curves, as seen in Fig. 3 and 4. There are several local maxima curves based on the P-V waveforms within the PS condition, but just a single global peak. Therefore, by operating PV systems at GM, the highest amount of solar energy may be gathered from the sun [26] [27].

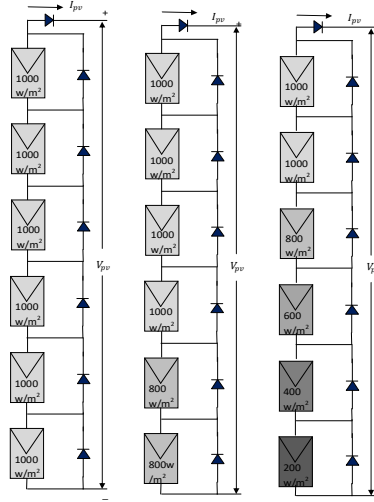


Fig. 2. Series linked PV array under uniform irradiance pattern

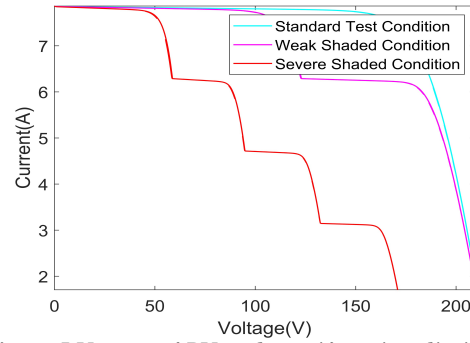


Fig. 3. I-V curve of PV under uniform irradiation

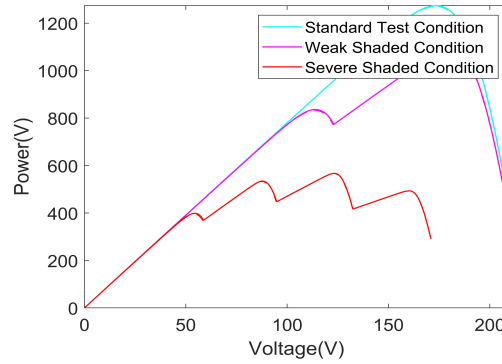


Fig. 4. P-V curve of PV under uniform irradiation

3.3 Boost Converter

A DC-DC boost converter, as shown in Fig. 3, serves as the connection between the PV panel and load to harvest the greatest amount of power from the panel and then supply it to the load [28]. Usually for MPPT operation, a control variable termed a duty cycle is measured by an MPPT controller that emits a control signal in the interval [0, 1]. From Eq. (5) to Eq. (8), the statistical framework is described.

$$V_o = \frac{V_i}{1 - D} \quad (5)$$

$$D = \frac{T_{on}}{T_{switch}} \quad (6)$$

$$L = \frac{D * (1 - D)^2 * R_{load}}{2 * f} \quad (7)$$

$$C_i = \frac{D}{8 * f^2 * L * 0.01} \quad (8)$$

$$C_o = \frac{d}{0.02 * f * R_{load}} \quad (9)$$

whereas V_o specify the output of the voltage, L is the inductor that minimizes the ripple current; V_o and V_i is the boost converter's input and output voltages; C_i state capacitor input and C_o specify the capacitor output congruently.

3.4 MPPT Controller

The appropriate MPPT controller is necessary to withdraw the obtained finest electric power by utilizing the solar systems. The PV array configuration makes use of MPPT technologies that maximise the power shading effect and are influenced by sun exposure characteristics such as temperature. Due to the continually shifting climate, the PV slope's MPP also changes. A controller needs to keep track of the MPP frequently and make adjustments. This type of controller or approach is known as MPPT techniques [29]. The MPP denotes the maximal point of a PV curve. MPP specifies the exact voltage and current that is present while the arrangement is in operation. To achieve this, MPPT adjusts the dynamic resistance output observed from the output terminals of the PV cell and feeds it up to the PI controller.

3.5 Proposed Methodology of MPPT

Solar energy is a long-lasting and essentially endless source of renewable energy. One of the most cost-effective and eco-friendly forms of energy is provided by PV systems that are powered by the sun. To address the challenge of monitoring a PV array's GP in partially shadowed situations (PSCs), the optimization-based MPPT methodology is implemented. This novel approach's main goal is to enhance the MPPT controller and boost converter for PV systems operating under partial shading based on the AVI-CO technique. Additionally, when an input with a lower DC voltage needs to be changed into an increased output DC voltage, high-power step-up DC-DC conversion infrastructure has grown more significant. Output voltage regulation in the DC-DC converter is achieved by adjusting the duty cycle with the help of the PI controller [30]. An improved approach termed the AVI-CO methodology is used to optimize the tuning of the PI controller gain dependent variables K_p and K_i . This method was designed by adopting the properties of the traditional optimization techniques for superior performance. In addition, the problem of monitoring a PV cell's GMP under PSCs is addressed using the AVI-CO based MPPT technique. The suggested framework is depicted schematically in Fig. 5.

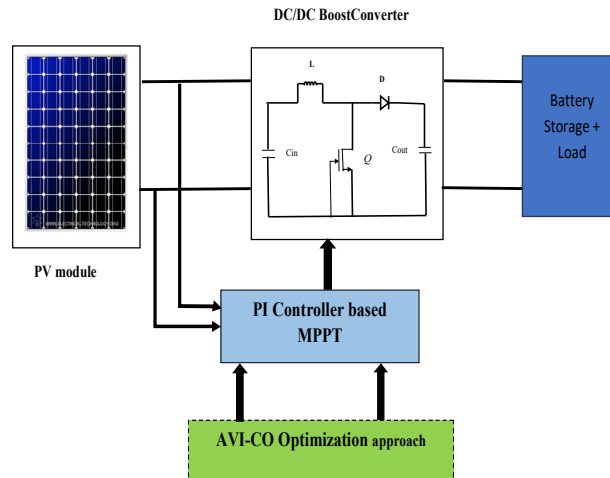


Fig. 5. Block diagram of proposed System

4. Finest Tuning of PI Attributes By Proposed AVI-CO Algorithm

4.1 Solution Encoding and Objective Function

For achieving optimal effectiveness, the PI controller is fed to the boost converter in which the presented work plans to tune the optimum PI variable quantities (K_p, K_i) respectively. As a result, the

recommended research explores the AVI-CO approach, which aids in producing global MPPT under PSC and therefore improves the SPV array's performance.

$$OF = \text{Max}(\text{efficiency}) \quad (10)$$

4.2 Adaptive Variable insisted Coyote Optimization (AVI-CO) Algorithm

A meta-heuristic technique called COA [31] has been employed in numerous fields of engineering. The coyote individuals were originally divided into $N_q \in n$ groups, each of which contained $N_{\text{coy}} \in n$ coyotes.

In the group, q every coyote dimension component might be changed in the following manner:

$$\text{SoC}_{\text{coy},j}^q = v_j^u + R_j (v_j^u - v_j^l) \quad (11)$$

Where, $\text{SoC}_{\text{coy},j}^q$ specifies the j^{th} dimensional attribute in the family q . v_j^u and v_j^l represents the top and bottom bounds within $[1, d]$; d implies the dimensional result within the interval $[0,1]$.

The growing process of coyotes was influenced by the graded arrangement (λ_1) and group culture (λ_2).

$$\lambda_1 = \alpha^q - \text{SoC}_{R_1}^q \quad (12)$$

$$\lambda_2 = \text{cul}^q - \text{SoC}_{R_2}^q \quad (13)$$

$$\text{SoC}_{\text{new}}^q = \text{SoC}^q + R_1 \lambda_1 + R_2 \lambda_2 + N \quad (14)$$

In the above eqn. (14) a variable ' N ' is introduced and is represented by

$$N = \text{floor}[(0.9 - R * 0.25 * M)] \quad (15)$$

Where, R defines the generated randomized count among $(0,1)$; $\text{floor}(\cdot)$ maps a realistic count to an integer count; M states the total coyote count. $\text{SoC}_{\text{new}}^q$ states the present result of the coyote in the family q ; R_1 and R_2 the arbitrary weights of λ_1 and λ_2 ranges within the bound $[0,1]$. cul^q defines the group's cultural tendency.

The COA only investigates the one alpha in this species that is best matched to the environment. Despite the packs, typically it contain two alphas [32][33]. The alpha of the q^{th} pack at the t point of time is well-defined in terms of an issue related to minimization as:

$$\alpha^{q,t} = \left\{ \text{SoC}^{q,t} \mid \arg_{c=\{1,2,\dots,N_{\text{coy}}\}} \min f(\text{SoC}^{q,t}) \right\} \quad (16)$$

$$\text{cul}_j^{q,t} = \begin{cases} \frac{H_{\frac{N_{\text{coy}}+1}{2},j}^{q,t}}{2} & N_{\text{coy}} \text{ is odd} \\ \frac{H_{\frac{N_{\text{coy}}}{2},j}^{q,t} + H_{\left(\frac{N_{\text{coy}}}{2}+1\right),j}^{q,t}}{2} & N_{\text{coy}} \text{ is even} \end{cases} \quad (17)$$

The coyote pattern is denoted by the term $H^{q,t}$ in the equation above, which is organized from low to high. The term $\text{cul}_j^{q,t}$ designates the cultural factor tendency of family q . Whenever the coyotes in their family reached adulthood, they decided to keep or get rid of growing coyotes in connection with equations (18) and (19).

$$\text{fitness}_{\text{new}}^q = f(\text{SoC}_{\text{new}}^q) \quad (18)$$

$$\text{SoC}_{\text{coy}}^q = \begin{cases} \text{SoC}_{\text{new}}^q, & \text{fitness}_{\text{new}}^q < \text{fitness}_{\text{coy}}^q \\ \text{SoC}_{\text{coy}}^q, & \text{fitness}_{\text{new}}^q \geq \text{fitness}_{\text{coy}}^q \end{cases} \quad (19)$$

Here, $\text{fitness}_{\text{new}}^q$ this signifies the present fitness value that can be achieved after the growth of coyote in the family q .

The birth and death of coyotes occur naturally. Recent genotypes can develop through mutation when the genes of infant coyotes are often obtained from arbitrary parents. The amount of inherited variation and dispersion probabilities are controlled by these two concepts.

$$P_{\text{scatter}} = \frac{1}{d} + C \quad (20)$$

Where, t defines the present iteration; $C_{\text{max}} = 1$; $C_{\text{min}} = 0.02$ and t_{max} be the maximal iteration count.

$$P_{\text{ass}} = \frac{(1 - P_{\text{scatter}})}{2} + C \quad (21)$$

In eq. (20) & (21) a variable 'C' is introduced and is given by

$$C = C_{\max} - t \left(\frac{C_{\max} - C_{\min}}{t_{\max}} \right) \quad (22)$$

The newly born coyote is expressed by,

$$\text{new_coyote}_j^q = \begin{cases} \text{SoC}_{R1,j}^q & R_j < P_{\text{scatter}} \text{ or } j = j_1 \\ \text{SoC}_{R2,j}^q & R_j \geq P_{\text{scatter}} + P_{\text{asso}} \text{ or } j = j_2 \\ r_j & \text{else} \end{cases} \quad (23)$$

Here, new_coyote_j^q specifies the j^{th} -dimensional attribute of newly born coyotes; j_1 and j_2 is the two arbitrary counts; r_j is the arbitrary solution of j^{th} dimensional attribute. P_{scatter} and P_{asso} be the scattered and associated probability.

Following the birth of pups, the group's lifespan and deaths were evaluated based on the aforementioned guidelines:

- The old coyote will die whereas the newly born coyote will remain alive unless a single coyote in a group is superior to the newborn coyote. At that time, the baby coyote's age is unknown.
- The oldest coyote kills if several coyotes are older than the current coyote. If multiple coyotes are of the same age, the worst coyote decreases. The young coyote lived and had an age of zero.
- The young coyotes will perish whenever the group's adult coyotes become healthier than their pups.

Coyotes in a family can dissolve their initial group and become autonomous earlier than randomly establishing additional groups. The tendency for coyotes to disregard their groups is indicated by,

$$P_{\text{evict}} = 0.005 N_{\text{coyo}}^2 \quad (24)$$

The coyotes' ages are increased by one when they are relocated and obtained, signifying the end of an iteration. Algorithm 1 describes the pseudocode of the adapted AVI-CO strategy. The AVI-CO mechanism's flow chart is shown in Fig. 6.

Algorithm 1: AVI-CO model	
<i>Step:1</i>	Initialize constraints N_{coyo} packs and N_q coyotes
<i>Step:2</i>	Assess the variances amongst every coyote
<i>Step:3</i>	While stopping criteria is unfulfilled do
<i>Step:4</i>	for every pack p do
<i>Step:5</i>	Calculate alpha pack from eqn. (16)
<i>Step:6</i>	Utilizing eqn. (16), ascertain the social tendencies
<i>Step:7</i>	for every c coyote do
<i>Step:8</i>	Upgrade social solution using eqn. (14)
<i>Step:9</i>	Evaluate present social solution using eqn. (18)
<i>Step:10</i>	Adaptation using eqn. (19)
<i>Step:11</i>	end for
<i>Step:12</i>	Simulate birth and death using eqn. (22)
<i>Step:13</i>	end for
<i>Step:14</i>	Implement coyote transitions amongst packs
<i>Step:15</i>	Upgrade age of each coyote
<i>Step:16</i>	End while
<i>Step:17</i>	Best coyote output

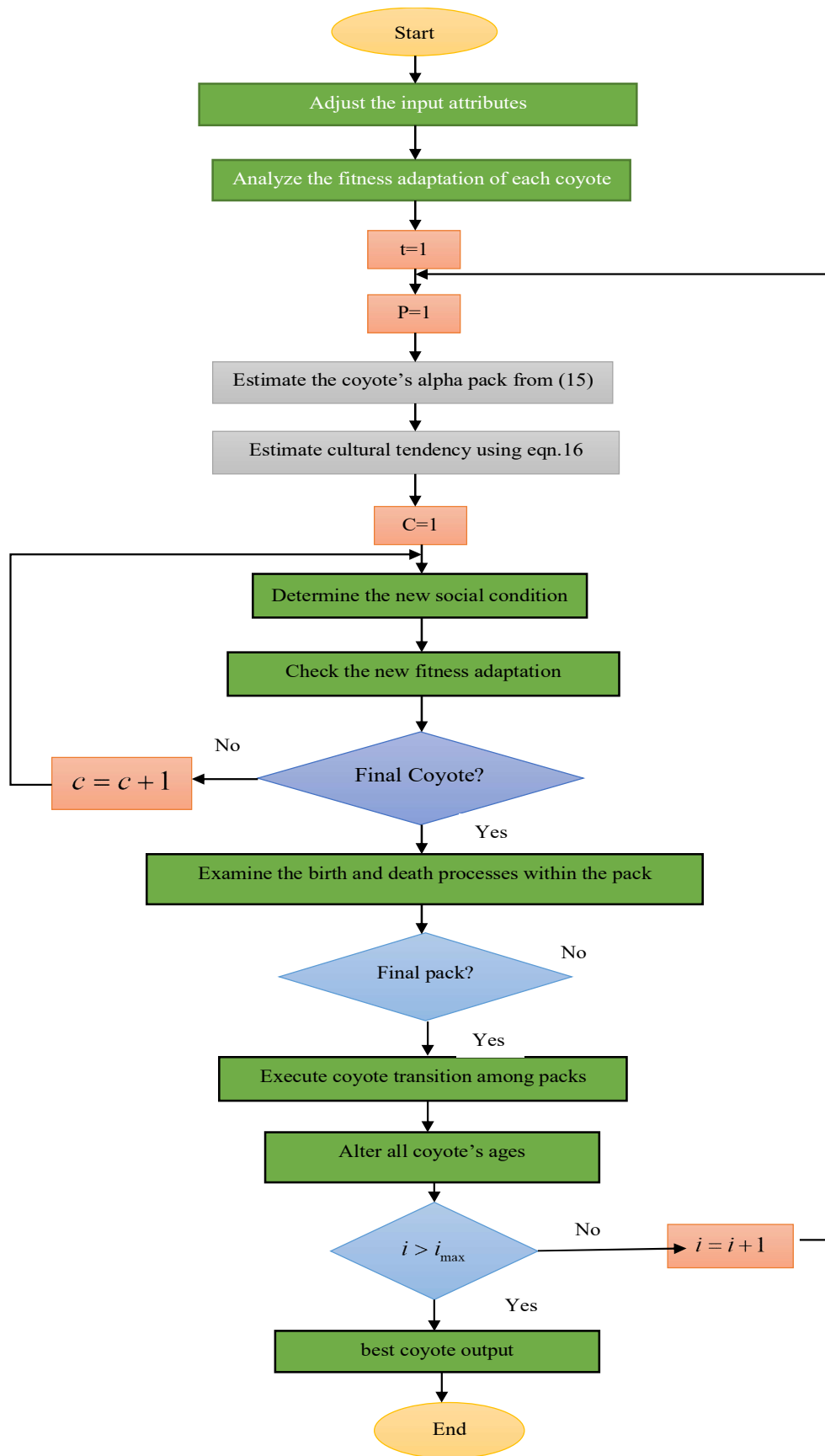


Fig. 6. Flowchart of AVI-CO approach

5. Results and Discussion

5.1 Simulation Procedure

In this simulated work, "Six PV panels connected in series" are employed to investigate the features of the PV array in circumstances with partial shading. Performance investigation was completed in MATLAB 2021b Simulink. The results obtained using the proposed approach are contrasted with those from traditional PSO [34] and WO algorithms to demonstrate the superiority of the suggested AVI-CO approach. Several MPPT techniques offer multiple tracking, speed and stable state effectiveness across every shaded pattern. The three shaded situations that are active for investigations were no shaded, Partially Shaded, and Fully Shaded conditions.

5.2 Analysis Under Different Scenarios

Case 1: No shaded Scenario

Fig. 7(a), (b) & (c) expose the graphic scrutiny of current, voltage and power tracked by MPT under PSC. All solar panels can be exposed to similar unchanging irradiation of (1000 W/m^2) and 25° C temperature. From the Figures, it seems that the current produced by the current AVI-CO scheme attains a steady state at 0.2s. In this instance, the power tracked by the existing methods, such as PSO, COA and WO achieve MPP with a tracking time of 0.42s, 0.52s and 0.12s. Formerly the proposed AVI-CO system reaches a higher power of 1300 W within 0.1s. Depending on the implemented outcomes, it is clear that the suggested AVI-CO reduces a tracking time of 76%, 80% and 16% compared to PSO, COA and WO-based tracking methods. Similarly, the presented AVI-CO approach attains a maximal voltage of 210V at time 0.2s, correspondingly.

Case 2: Partially Shaded Scenario

For a PV array with 25° C temperature, this set-up takes solar radioactivity of 1000 kW/m^2 , 1000 kW/m^2 , 1000 kW/m^2 , 800 kW/m^2 , and 800 kW/m^2 into account. Fig. 8 (a), (b) and (c) displays the wave pattern of the current, voltage, and power during the partial test conditions. The reported maximum tracking power for the existing methods, such as PSO, COA, and WO occurs at 0.2 seconds, 0.22 seconds, and 0.14 seconds. However, the recommended AVI-CO method manages to reach its 1100W maximum output at 0.12s. According to the findings of the implementation, the suggested AVI-CO reduces tracking time by 40%, 45.5%, and 14.28%. It is compared to PSO, COA, and WO-based tracking methods discretely. Additionally, the demonstrated AVI-CO technique achieves a maximum voltage of 210V at a tracking time of 0.2s.

Case 3: Fully shaded Scenario

In this case, PV modules are exposed to solar radioactivity of 1000 kW/m^2 , 1000 kW/m^2 , 800 kW/m^2 , 600 kW/m^2 , 400 kW/m^2 , and 200 kW/m^2 with 25° C temperature. The power, current and voltage curves of the suggested approaches compared to the current ones under rigorous test conditions are shown in Figs.9 (a), (b) and (c) in terms of time. The prevailing methods such as PSO, COA, and WO achieve their maximum power with a tracking period of 0.18, 0.12, and 0.22 seconds. The newly developed AVI-CO technique reaches an extreme power of 600W in 0.1s. According to the simulation results, the provided AVI-CO arrangement decreases its time of tracking by 50%, 44%, and 16% in contrast to CSO, HBA, and WO-based tracking approaches.

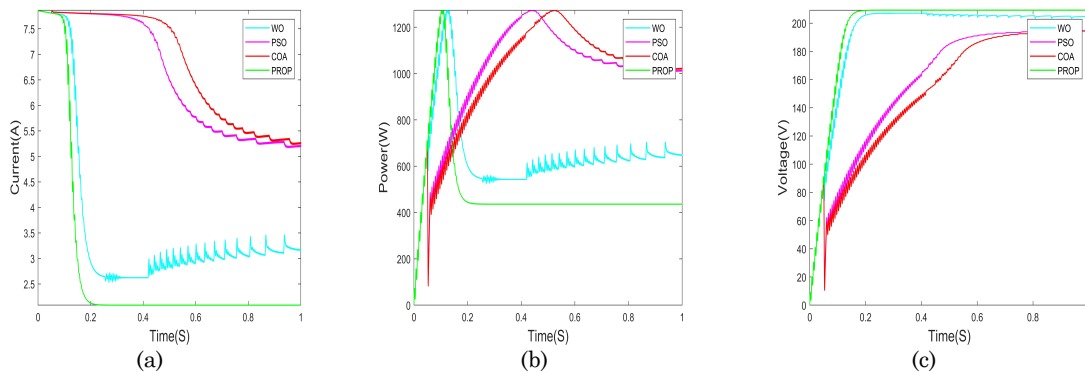


Fig. 7. Graphic study of Current, Voltage and Power under no-shaded scenario

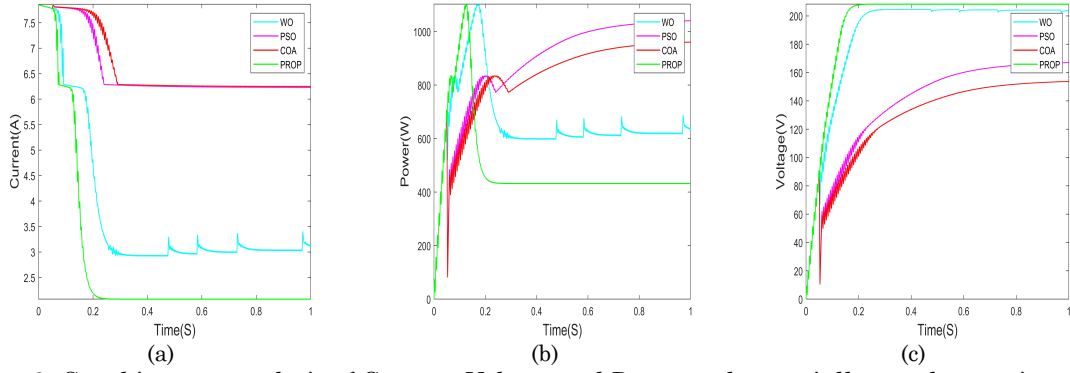


Fig. 8. Graphic curve analysis of Current, Voltage and Power under partially tested scenarios

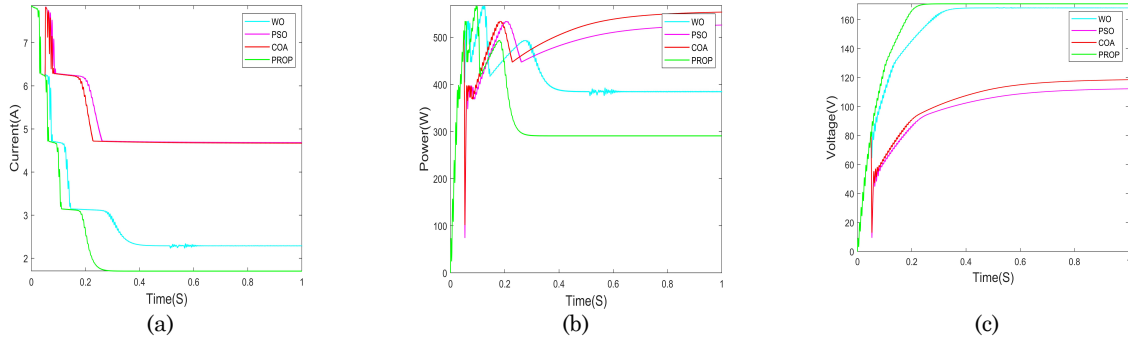


Fig. 9. Graphic wave pattern of power, voltage and current under fully shaded scenario

5.3 Convergence Analysis

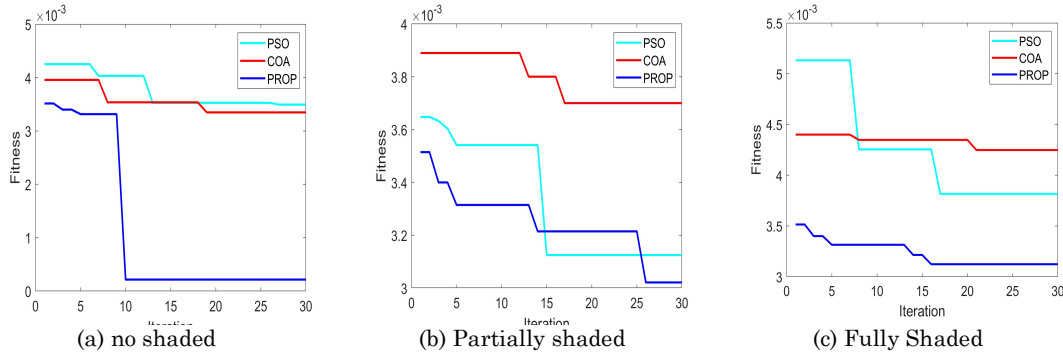


Fig. 10. Converging graph of developed over prevailed techniques under PSC

Fig. 10 demonstrates a comparative analysis of the adapted scheme to prevailing schemes with cost functions under PSCs. Here, the number of iterations such as 5, 10, 15, 20, 25 and 30 are observed. The concluded findings of the convergence graph make it obvious that the created AVI-CO system constantly produces lower cost rate values in contrast with the standard methods. On considering the proposed AVI-CO strategy with the existing scheme under unshaded conditions, the proposed approach converges quicker and also attains a cost value of 0.2 at the 20th iteration. The cost function of the typical technique is 3.56 for PSO schemes and 3.9 for the COA approach at the 10th iteration. The suggested system obtains a minimal cost of 3.32 during partially shaded scenarios that coincide quickly with alternative strategies. When contrasted with previous methods under fully shaded test conditions, the new system converges more quickly at the 25th iteration, with a cost value of 3.1. Hence, the recommended method is found to satisfy the requirement of a quick dynamic response from the simulated process.

5.4 Best Parameter Investigation

The PI controllers have an abundance of major shortcomings, which can be rectified through the modifications of the gain attributes like K_p and K_i . To change these constraints, a time-consuming trial-and-error approach is frequently employed. In this proposed mode, the AVI-CO approach is developed to modify the PI controller's parameters. Table 2 displays the calculated ideal parameter values for the

standard, weak, and severe test situations. The adapted AVI-CO methodology is also validated by employing the prevalent technologies including WO, CSO, and HBA.

Table 2: Optimum parameter values for Cases 1, 2 and 3

	Parameters	WO	PSO	COA	PROP
Case 1	K _P	0.2	0.42153	0.15315	0.2345
	K _I	0.2	0.00326	1.1012	1.2325
Case 2	K _P	0.2	0.62544	0.21548	0.0045
	K _I	0.2	0.16586	0.1815	0.03264
Case 3	K _P	0.2	0.0545	0.0565	0.11212
	K _I	0.2	0.2327	0.1742	0.13526

5.5 Analysis of Efficiency

Table 3 displays the effectiveness assessment of the hybrid technique for each of the three circumstances, which are standard, weak, and severe, respectively. The table below makes clear that the established plan is more effective than the practices currently in use. The proposed plan has 97.22% efficiency under no-shaded circumstances. In the light-shaded condition, the recommended AVI-CO technique achieves 98.85% efficiency. While in the severe-shaded state, it achieves 98.10% efficiency.

Table 3: Efficacy analysis under partial shading conditions

	WO	PSO	COA	PROP
Standard condition	81.021	90.948	92.404	97.221
Weak shaded	95.297	93.87	94.542	98.851
Severe shaded	83.566	90.274	94.874	98.102

5.6 Stability Analysis

The stability investigation of the newly introduced system compared with the typical approach under various shading situations is shown in Tables 4, 5 and 6. Considering Table 4, it seems that the created AVI-CO approach settles in 709095.69 seconds, whereas typical methods like PSO and WO methods accomplish 620041.37 and 170598.74 seconds, subsequently. Likewise, the settling maximum value of standard PSO achieves 194.87 and WO achieves 207.45 while the new AVI-CO strategy achieves 194.52, which provide superior result compared to other approaches. By comparing the executed model to typical techniques, the findings demonstrate that the presented model achieves the largest settling value. Additionally, the created scheme's minimal settling value is 174.68, whereas the corresponding conventional approaches get 175.00 for PSO and 184.34 without optimization. Hence, the better-quality results determine the value of the suggested AVI-CO strategy.

Table 4: Stability Analysis for case 1

	WO	PSO	PROP
Rise Time	128418.94	448018.84	530920.81
Settling Time	170598.74	620041.37	709095.69
Settling Min	184.3418	175.001	174.687
Settling Max	207.4594	194.8771	194.524
Overshoot	1.2882	0.0923	0.08027
Undershoot	0	0	0
Peak	207.459	194.877	194.524
Peak Time	274601	1024663	1039096

Table 5: Stability Analysis for Case 2

	WO	PSO	PROP
Rise Time	162575.45	452314.45	454659.54
Settling Time	220737.42	751997.63	761532.48
Settling Min	181.6675	150.089	138.116
Settling Max	204.678	167.194	153.894
Overshoot	0.4463	0.0817	0.09650
Undershoot	0	0	0
Peak	204.678	167.194	153.8944
Peak Time	482226	1042445	1044646

Table 6: Stability Analysis for Case 3

	WO	PSO	PROP
Rise Time	222474.81	366740.42	383155.45
Settling Time	313999.26	699398.61	692222.70
Settling Min	151.117	110.86	106.51
Settling Max	168.43	112.41	118.68
Overshoot	0.1749	0.10151	0.0912
Undershoot	0	0	0
Peak	168.43	112.41	118.68
Peak Time	520123	1045797	1059633

6. Advantages and Disadvantages

Advantages

- PI controller was able to reach the MPP quickly and oscillation is close to zero.
- The suggested method creates cleaner air because of its quick tracking capabilities, increased power efficacy, and high energy harvesting.
- The suggested method track GMPP with higher efficacy.

Disadvantages

- The suggested approach has a major drawback of complicated calculation process. Thus, it has not been widely applied for other problems regarding distribution networks.
- The main drawback of MPPT charge controllers is that they are more expensive and complex than PWM charge controllers, as they require more components and circuitry to perform the DC-DC conversion and the power tracking.

7. Conclusion

This paper implemented an innovative AVI-CO methodology for optimizing the MPPT controller's performance in PV systems at PSC. The newly invented method's main objective is to measure the solar energies MPP under partial shading scenarios. To regulate the voltage that comes out of a DC-DC converter, a PI controller's duty cycle must be varied. The recommended AVI-CO technique is used to optimize the PI controller coefficients K_p and K_i for enhanced performance. In addition to carrying out the investigational research, the adapted work is implemented in MATLAB/Simulink. By contrasting the results of the AVI-CO-based MPPT and Boost converter model with those of the traditional approaches. The performance of the proposed model is then verified. On considering the proposed AVI-CO strategy with the existing scheme under unshaded conditions, it converges superior and achieves a cost value of 0.2 at the 20th iteration. Nevertheless, the cost function of the current technique is 3.56 for PSO models and 3.9 for the COA scheme at the 10th iteration. The suggested approach obtains a cost rate of 3.32 during partially shaded scenarios that coincide quickly with alternative strategies. Moreover, the suggested plan has 97.22% efficiency under no-shaded circumstances. In the light-shaded condition, the recommended AVI-CO technique achieves a 98.85% efficiency in the severe-shaded state. When compared to WO, PSO and COA, we obtained an accuracy of 98.10% efficiency. A statistical study demonstrates that the recommended strategies are more stable and robust than the alternatives. The suggested method creates cleaner air because of its quick tracking capabilities, increased power efficacy, and high energy harvesting.

Compliance with Ethical Standards

Conflicts of interest: Authors declared that they have no conflict of interest.

Human participants: The conducted research follows the ethical standards and the authors ensured that they have not conducted any studies with human participants or animals.

References

- [1] A. M. Eltamaly and A. Y. Abdelaziz (eds.), "Modern Maximum Power Point Tracking Techniques for Photovoltaic Energy Systems," Green Energy and Technology, 2020.
- [2] E. H. Houssein, M. A. Mahdy, A. Fathy and H. Rezk, "A modified Marine Predator Algorithm based on opposition based learning for tracking the global MPP of shaded PV system," Expert Systems with Applications, 2021.
- [3] I. Shams, S. Mekhilef and K. S. Tey, "Maximum Power Point Tracking Using Modified Butterfly Optimization Algorithm for Partial Shading, Uniform Shading, and Fast Varying Load Conditions," in IEEE Transactions on Power Electronics, Vol. 36, No. 5, pp. 5569-5581, 2021.
- [4] N. Padmavathi, A. Chilambuchelvan and N. R. Shanker, "Maximum Power Point Tracking During Partial Shading Effect in PV System Using Machine Learning Regression Controller," J. Electr. Eng. Technol, Vol. 16, pp. 737-748, 2021.
- [5] Zafar, Muhammad & Alshahrani, Thamraa & Khan, Noman & Mirza, Adeel & Mansoor, Majad & Qadir, Muhammad & Khan, Muhammad Imran & Naqvi, Rizwan, "Group Teaching Optimization Algorithm Based MPPT Control of PV Systems under Partial Shading and Complex Partial Shading," Electronics, Vol. 9. pp. 1962, 2020.
- [6] Rocha, Maykon & Sampaio, Leonardo & Oliveira da Silva, Sergio, "Comparative Analysis of MPPT Algorithms Based on Bat Algorithm for PV Systems Under Partial Shading Condition," Sustainable Energy Technologies and Assessments, Vol. 40. pp. 1-14, 2020.
- [7] Zafar, Muhammad & Khan, Noman & Mirza, Adeel & Mansoor, Majad, "Bio-Inspired Optimization Algorithms Based Maximum Power Point Tracking Technique for Photovoltaic Systems under Partial Shading and Complex Partial Shading Conditions," Journal of Cleaner Production, Vol. 309, pp. 127279, 2021.
- [8] N. Mujeeb Khan, U. Amir Khan and M. Hamza Zafar, "Maximum Power Point Tracking of PV System under Uniform Irradiance and Partial Shading Conditions using Machine Learning Algorithm Trained by Sailfish Optimizer," 2021 4th International Conference on Energy Conservation and Efficiency (ICECE), Lahore, Pakistan, pp. 1-6, 2021.
- [9] T. W. BANK. "Population growth (annual %)". [online]. Available: <https://data.worldbank.org/indicator/SP.POP.GROW>
- [10] I. Capellán-Pérez, M. Mediavilla, C. de Castro, Ó. Carpintero, and L. Miguel, "Fossil fuel depletion and socio-economic scenarios: An integrated approach", vol. In Press, 2014. [online]. Available: <https://www.sciencedirect.com/science/article/pii/S0360544214011219>
- [11] H. S. Aanesan K, Pinner D., "Solar power. Darkest before dawn,". [online]. (2017) Available: <https://www.semanticscholar.org/paper/Solar-power%3A-Darkest-before-dawn-Aanesen-Heck/e42c56b0be121dc5aa89086384fe69757afedcb3>.
- [12] F. B., "Mid-term renewable energy market report," 2015. [online]. Available: <https://www.iea.org/reports/medium-term-renewable-energy-market-report-2015>
- [13] Z. Q. Wu and D. Q. Yu, "Application of improved bat algorithm for solar PV maximum power point tracking under partially shaded condition," Applied Soft Computing, Vol. 62, pp. 101-109, 2018.
- [14] A. Bidram, A. Davoudi, and R. S. Balog, "Control and Circuit Techniques to Mitigate Partial Shading Effects in Photovoltaic Arrays," IEEE Journal of Photovoltaics, Vol. 2, pp. 532-546, 2012.
- [15] A. Maki and S. Valkealahti, "Power Losses in Long String and Parallel Connected Short Strings of Series-Connected Silicon-Based Photovoltaic Modules Due to Partial Shading Conditions," IEEE Transactions on Energy Conversion, Vol. 27, pp. 173-183, 2012.
- [16] H. L. Jou, K. D. Wu, J. C. Wu, C. H. Chung, and D. F. Huang, "Voltage Equalizing of Solar Modules for Shadowing Compensation," Journal of Power Electronics, Vol. 17, pp. 514-521, 2017.
- [17] D. Pilakkat and S. Kanthalakshmi, "An improved P&O algorithm integrated with artificial bee colony for photovoltaic systems under partial shading conditions," Solar Energy, Vol. 178, pp. 37-47, 2019.
- [18] R. Ahmad, A. F. Murtaza, and H. A. Sher, "Power tracking techniques for efficient operation of photovoltaic array in solar applications - A review," Renewable & Sustainable Energy Reviews, Vol. 101, pp. 82- 102, 2019.
- [19] N. Kumar, I. Hussain, B. Singh and B. K. Panigrahi, "Maximum Power Peak Detection of Partially Shaded PV Panel by Using Intelligent Monkey King Evolution Algorithm," IEEE Transactions on Industry Applications, vol. 53, pp. 5734-5743, 2017.
- [20] M. Seyedmahmoudian, T. K. Soon, B. Horan, A. Ghandhari, S. Mekhilef, and A. Stojcevski, "New ARMO-based MPPT Technique to Minimize Tracking Time and Fluctuation at Output of PV Systems under Rapidly Changing Shading Conditions," IEEE Transactions on Industrial Informatics, pp. 1-1, 2019.
- [25] N. Anani, H. Ibrahim, "Adjusting the single-diode model parameters of a photovoltaic module with irradiance and temperature," Energies, Vol. 13, No. 12, pp. 3226, 2020.
- [26] H. Hanifi, et al., "A novel electrical approach to protect PV modules under various partial shading situations," Sol. Energy, Vol. 193, pp. 814-819, 2019.
- [27] Z. Alqaisi, Y. Mahmoud, "Comprehensive study of partially shaded PV modules with overlapping diodes," IEEE Access, Vol. 7, pp. 172665-172675, 2019.
- [28] P. Shaw, "Modelling and analysis of an analogue MPPT-based PV battery charging system utilising dc-dc boost converter," IET Renew. Power Gener, Vol. 13, No. 11, pp. 1958-1967, 2019.
- [29] Pathak, Diwaker, G. Sagar and P. Gaur, "An application of intelligent non-linear discrete-PID controller for MPPT of PV system." Procedia Computer Science, Vol. 167, pp. 1574-1583, 2020.

- [30] Islam, Haidar, S. Mekhilef, N. M. Shah, T. K. Soon, A. Wahyudie and M. Ahmed, "Improved Proportional-Integral Coordinated MPPT Controller with Fast Tracking Speed for Grid-Tied PV Systems under Partially Shaded Conditions" *Sustainability*, Vol. 13, No. 2, pp. 830, 2021.
- [31] J. Pierezan and L. Dos Santos Coelho, "Coyote Optimization Algorithm: A New Metaheuristic for Global Optimization Problems," 2018 IEEE Congress on Evolutionary Computation (CEC), Rio de Janeiro, Brazil, pp. 1-8, 2018.
- [32] S. A. Poessel, E. M. Gese and J. K. Young, "Influence of habitat structure and food on patch choice of captive coyotes," *Applied Animal Behaviour Science*, Vol. 157, pp. 127-136, 2014.
- [33] E. M. Gese, R. L. Ruff and R. L. Crabtree, "Foraging ecology of coyotes (*Canis latrans*): the influence of extrinsic factors and a dominance hierarchy," *Canadian Journal of Zoology*, Vol. 74, No. 5, pp. 769-783, 1996.
- [34] A. G. Gad, "Particle Swarm Optimization Algorithm and Its Applications: A Systematic Review," *Arch Computat Methods Eng*, Vol. 29, pp. 2531-2561, 2022.